

Are your **MRI contrast agents** cost-effective?

Learn more about generic **Gadolinium-Based Contrast Agents**.



**AJNR**

**Clinical Evaluation of Reduced Field-of-View Diffusion-Weighted Imaging of the Cervical and Thoracic Spine and Spinal Cord**

J.B. Andre, G. Zaharchuk, E. Saritas, S. Komakula, A. Shankaranarayan, S. Banerjee, J. Rosenberg, D.G. Nishimura and N.J. Fischbein

This information is current as of April 17, 2024.

*AJNR Am J Neuroradiol* 2012, 33 (10) 1860-1866

doi: <https://doi.org/10.3174/ajnr.A3134>

<http://www.ajnr.org/content/33/10/1860>

**ORIGINAL  
RESEARCH**

J.B. Andre  
G. Zaharchuk  
E. Saritas  
S. Komakula  
A. Shankaranarayan  
S. Banerjee  
J. Rosenberg  
D.G. Nishimura  
N.J. Fischbein

# Clinical Evaluation of Reduced Field-of-View Diffusion-Weighted Imaging of the Cervical and Thoracic Spine and Spinal Cord

**BACKGROUND AND PURPOSE:** DWI has the potential to improve the detection and evaluation of spine and spinal cord pathologies. This study assessed whether a recently described method (rFOV DWI) adds diagnostic value in clinical patients.

**MATERIALS AND METHODS:** Consecutive patients undergoing clinically indicated cervical and/or thoracic spine imaging received standard anatomic sequences supplemented with sagittal rFOV DWI by using a b-value of 500 s/mm<sup>2</sup>. Two neuroradiologists blinded to clinical history evaluated the standard anatomic sequences only for pathology and provided their level of confidence in their diagnosis. These readers then rescored the examinations after reviewing the rFOV DWI study and indicated whether this sequence altered findings or confidence levels.

**RESULTS:** Two hundred twenty-three patients were included in this study. One hundred eighty patient scans (80.7%) demonstrated at least 1 pathologic finding. Interobserver agreement for identifying pathology ( $\kappa = 0.77$ ) and in assessing the added value of the rFOV DWI sequence ( $\kappa = 0.77$ ) was high. In pathologic cases, the rFOV DWI sequence added clinical utility in 33% of cases ( $P < .00001$ , Fisher exact test). The rFOV DWI sequence was found to be helpful in the evaluation of acute infarction, demyelination, infection, neoplasm, and intradural and epidural collections ( $P < .001$ ,  $\chi^2$  test) and provided a significant increase in clinical confidence in the evaluation of 11 of the 15 pathologic subtypes assessed ( $P < .05$ , 1-sided paired Wilcoxon test).

**CONCLUSIONS:** rFOV diffusion-weighted imaging of the cervical and thoracic spine is feasible in a clinical population and increases clinical confidence in the diagnosis of numerous common spinal pathologies.

**ABBREVIATIONS:** CI = confidence interval; rFOV = reduced field-of-view; SS-EPI = single-shot EPI; STIR = short-tau inversion recovery

The diffusion of water molecules in biologic tissues is altered in numerous pathologic processes.<sup>1-3</sup> While imaging changes in diffusion have found their greatest clinical utility in the assessment of the human brain, the spine and spinal cord could also benefit from diffusion imaging. Because of the small size of the spinal cord and other technical challenges related to spine imaging, DWI is less often performed for these examinations.<sup>4-8</sup> Traditionally SS-EPI schemes have been used to perform DWI, but they are prone to geometric distortion primarily in the phase-encode direction secondary to long read-out times and low bandwidth. Advanced EPI-based techniques have thus been developed to address this issue, including interleaved (or multishot) EPI<sup>7,9,10</sup> and parallel imaging.<sup>11-13</sup> However, these techniques also have shortcomings,<sup>14</sup> and this has limited clinical diffusion-weighted imaging of the spine and spinal cord.

A reduced field-of-view methodology with or without outer volume suppression for DWI of the spinal cord and column has been developed recently.<sup>14-17</sup> This technique is attractive because of the inherent geometry of the spinal cord, which allows significant reduction in the anteroposterior di-

mension of the imaging volume, thus significantly reducing the above-mentioned distortion. It has been recently demonstrated that the rFOV technique improves image quality, is preferred over conventional full-FOV SS-EPI across multiple imaging metrics, and is feasible in a clinical setting.<sup>14</sup> Moreover, other studies have suggested that the addition of a DWI sequence to conventional imaging of the spine may provide added clinical value, including the ability to more accurately differentiate degenerative disk disease from diskitis and benign from malignant compression fractures.<sup>18-23</sup>

In this study, we performed an rFOV EPI-based diffusion-weighted sequence on an unselected group of clinical patients undergoing clinically indicated imaging of the spine. We assessed whether it improved visualization of specific pathologies, narrowed the differential diagnosis for any findings, and/or increased diagnostic confidence.

## Materials and Methods

### Industrial Support

The pulse sequence used for this research is a collaborative “work-in-progress” between Stanford University and GE Healthcare.

### Patient Population

Patients provided informed consent for this prospective study approved by our institutional review board. Consecutive patients undergoing clinically indicated cervical, thoracic, or full-spine imaging on a 1.5T scanner with an adequate slew rate (defined below) and

Received November 18, 2011; accepted after revision February 13, 2012.

From the Departments of Radiology (J.B.A., G.Z., S.K., J.R., N.J.F.) and Electrical Engineering (E.S., D.G.N.), Stanford University, Stanford, California; and Applied Sciences Laboratory-West (A.S., S.B.), GE Healthcare, Menlo Park, California.

Please address correspondence to Jalal B. Andre, MD, University of Washington, 1959 NE Pacific St. NW011, Box 357115, Seattle, WA 98195-7115; e-mail: drjalal@uw.edu

<http://dx.doi.org/10.3174/ajnr.A3134>

imaged between March 2008 and August 2010 were eligible for inclusion into this study. Exclusion criteria were nondiagnostic examinations due to patient motion, technical factors, and/or extensive surgical hardware (the latter resulting in severe geometric distortion in the rFOV DWI). Finally, only a relatively small number of lumbar spine examinations included the rFOV DWI technique during this time (13 in total) because our investigation was focused mainly on the spinal cord, and hence these were excluded from the study.

### Imaging Methods

Four different 1.5T MR imaging scanners were used (Signa; GE Healthcare, Milwaukee, Wisconsin) with 40 mT/m maximum gradient strength and 150 mT/m/ms maximum slew rate at 2 inpatient and 2 outpatient settings. All studies used body coil transmission and an 8-channel cervical-thoracic-lumbar coil for signal reception. All patients received standard anatomic imaging, which, at our institution, includes a 3-plane single-shot FSE T2-weighted localizer, sagittal T1-weighted spin-echo (TR/TE, 500/22 ms), sagittal T2-weighted FSE (TR/TE, 2400/115 ms), and axial T2-weighted FSE (TR/TE, 4500/103 ms). Cervical spine examinations also routinely include sagittal STIR (TR/TE/TI, 4615/50/140 ms) and axial gradient-echo (TR/TE, 475/11 ms) images. These latter sequences were variably included in thoracic and/or full spine examinations, as per clinical indication. Postcontrast T1-weighted sagittal (TR/TE, 650/22 ms) and axial (TR/TE 500/8 ms) imaging with fat-suppression was performed in patients with appropriate indications following injection of 0.1 mmol/kg of gadolinium-based contrast agent.

rFOV DWI was acquired in the sagittal plane using a 90° 2D echo-planar radio-frequency excitation followed by a 180° refocusing pulse.<sup>14,16</sup> The TR/TE/EPI readout time was 3600/69/54 ms, with a bandwidth of 62.5 kHz. B0 images and  $b = 500$  s/mm<sup>2</sup> images were acquired, the latter in 3 orthogonal planes. Six 4-mm sections with no intersection gap were obtained. In-plane spatial resolution was constant for all examinations at 0.94 mm<sup>2</sup>. The cervical spine examinations used an rFOV measuring 4.5 × 18 cm, with a matrix of 48 × 192, while the thoracic and full spine studies used an rFOV measuring 6 × 30 cm, with a matrix of 64 × 320. Total imaging time was 2 minutes, 30 seconds. Postprocessing software automatically produced isotropic DWI and ADC images. No cardiac or respiratory gating was performed.

### Radiologic Assessment

Two neuroradiologists (N.J.F., S.K.), blinded to all patient identifiers and clinical data (including presentation, symptoms, history, and indication for imaging), first evaluated only the standard anatomic sequences (ie, without access to the rFOV sequence) for the presence of typical spinal pathologies within the extradural, intradural extramedullary, and intramedullary spaces. Fifteen prespecified pathologies relating to each of these compartments were defined as follows—extradural space (epidural space, vertebral column, and prevertebral space): trauma, mass (neoplasm), infection, disk herniation/degenerative disk disease; intradural extramedullary space: mass (neoplasm), hemorrhage, fluid collection (nonhemorrhagic); and intramedullary space: demyelination, infarction, infection, mass (neoplasm), syrinx, contusion, hemorrhage, and vascular malformation. Allowance was made for expert reader identification of additional pathologies within each of these 3 compartments, as appropriate, though this was rarely needed. The readers were asked to state a level of confidence in their diagnosis on a 3-point scale (1 = lowest, 3 = highest).

Readers were then asked to rescore the examinations after review-

ing the rFOV DWI sequence and to restate a level of confidence in their diagnosis by using the same 3-point scale. Additionally, readers were asked whether they thought that the rFOV DWI sequence added clinical utility, defined as the following: 1) helping to confirm or substantiate the findings identified on conventional sequences, 2) helping to narrow the differential diagnosis, and/or 3) helping to exclude  $\geq 1$  initially considered alternative pathology. For cases in which the rFOV DWI sequence provided added clinical utility, readers were asked whether the DWI sequence supported or excluded a suggested pathology or assisted in narrowing the differential diagnosis. At a later interpretation session, disagreements in diagnosis were resolved by consensus.

### Statistical Analysis

A biostatistician (J.R.) performed all statistical analyses by using STATA, Release 9.2, software (StataCorp, College Station, Texas). Expert reader agreement was calculated with an unweighted  $\kappa$ , with confidence intervals based on 1000 bootstrap replications and the exact Bowker test of symmetry. Change in confidence in a given diagnosis was tested with a 1-sided paired Wilcoxon test and considered significant with  $P$  values  $< .05$ . A  $\chi^2$  test was performed to evaluate whether the proportion of cases in which rFOV DWI was thought to be clinically useful was uniform across all pathologies evaluated.

### Results

Two hundred forty-six patients were initially imaged with the rFOV DWI sequence. Of these, 16 were excluded secondary to significant patient motion, technical difficulties, and/or excessive surgical hardware. An additional 7 patients underwent dedicated lumbar spine examinations and were subsequently excluded due to the relatively small number of examinations covering this anatomic location. Thus, 223 patients (116 women, 107 men; mean age, 51 ± 45 years; range, 11–92 years) met the inclusion criteria and are included in this study. The clinical indications for imaging were the following: post-trauma,  $n = 62$ ; weakness,  $n = 32$ ; neck/back pain,  $n = 28$ ; known or suspected neoplasm,  $n = 24$ ; combined motor and sensory abnormalities,  $n = 22$ ; known or suspected infection,  $n = 18$ ; sensory abnormalities,  $n = 15$ ; postsurgical examination,  $n = 10$ ; follow-up of incidental findings on a prior examination,  $n = 8$ ; and neurodegenerative disease,  $n = 4$ . Imaged anatomy included 166 cervical, 18 combined cervical and thoracic, 33 thoracic, 3 combined thoracic and lumbar, and 3 full spine examinations for a total of 185 cervical and 55 thoracic spine examinations.

One hundred eighty patient scans (80.7%) demonstrated at least 1 pathology, as determined by consensus read (Table 1). Interobserver agreement was substantial in identifying pathology on routine anatomic images ( $\kappa = 0.77$ ), presented in Table 2. Overall agreement between readers in assessing diagnostic confidence on these images was moderate, with unweighted  $\kappa = 0.57$  and Bowker test of symmetry  $P$  value  $< .0001$  (indicating that 1 reader routinely gave higher diagnostic confidence scores). While agreement between readers in assessing diagnostic confidence by using the rFOV DWI sequence was lower ( $\kappa = 0.33$  [95% CI = 0.21–0.45;  $P < .0001$ ]), agreement regarding the added value of the rFOV DWI sequence was high ( $\kappa = 0.77$  [95% CI = 0.70–0.83;  $P < .0001$ ]), as illustrated in Table 2. In patients with concern for pathology based on routine anatomic MR images, the rFOV

**Table 1: Spinal pathologies included in the current study**

Spinal Pathology	Total Cases	Paired Wilcoxon Test
		Increased Confidence with Added DWI (P value) <sup>a</sup>
Trauma (extradural) <sup>b</sup>	28	.0005
Neoplasm (extradural) <sup>b</sup>	16	.0047
Infection (all locations) <sup>b</sup>	14	<.0001
Disk herniation	112	.1573
Mass (intradural extramedullary) <sup>b</sup>	4	.0455
Mass (intramedullary) <sup>b</sup>	4	.0253
Hemorrhage (intradural extramedullary) <sup>b</sup>	2	.0143
Hemorrhage (intramedullary)	2	.3173
Collection (intradural extramedullary) <sup>b</sup>	4	.0003
Demyelination <sup>b</sup>	20	<.0001
Cord infarction <sup>b</sup>	6	<.0001
Syrinx	3	.0833
Cord contusion <sup>b</sup>	23	<.0001
Vascular malformation	1	.1573
No radiologic evidence of pathology	48	N/A

<sup>a</sup> P values represent the paired Wilcoxon test for the presence of a change in clinical confidence for a given diagnosis on the addition of the rFOV DWI sequence.

<sup>b</sup> Significant at the  $P < .05$  level.

DWI sequence was found to be of added clinical utility in 33% of cases ( $P < .00001$ , Fisher exact test). In cases without pathology, there was no added value.

Of the initially considered differential possibilities identified on conventional sequences, a total of 117 initial pathologic entities were excluded after review of the rFOV DWI sequence, while 97 pathologic entities were further suggested or at times “newly suggested.” For all pathologies, rFOV DWI had an impact regarding a change in diagnosis ( $P < .0001$ , 1-sided paired Wilcoxon test). Among specific pathologies, the rFOV DWI sequence was found to be most helpful in the evaluation of acute infarction, demyelination, infection, neoplasm, and intradural and epidural collections ( $P < .001$ ,  $\chi^2$  test). Following rFOV DWI review, clinical confidence scores increased for 11 of the 15 pathologic subtypes (Table 1). The rFOV DWI sequence did not add clinical utility in the evaluation of disk herniation/degenerative disk disease, intramedullary vascular malformations (1 case), intramedullary hemorrhage (2 cases), or syrinx (3 cases), but all of these pathologies except disk disease were present in very low numbers. In 45 cases, after review of the rFOV DWI sequence, the differential diagnosis of 1 of the readers was narrowed to a single possible pathology or completely excluded all initially considered pathologies.

An example of the added value of the rFOV DWI sequence in the evaluation of acute spinal cord infarction is given in Fig 1. The rFOV diffusion images can also be of added clinical value in detecting incidental but potentially significant findings as demonstrated in Fig 2, a patient with a spinal cord infarct and a schwannoma that was difficult to appreciate on the conventional anatomic MR images only. Figure 3 shows a case of spinal neoplasm in which the hypercellular nature of the dorsal epidural mass and multiple additional hypercellular bony lesions (later biopsy-proved lymphoma) are nicely depicted on the rFOV DWI. Examples of spinal trauma and spinal cord abscess are shown in Figs 4 and 5, respectively.

## Discussion

The rFOV DWI technique has previously been shown to produce qualitatively superior images compared with routine “full-FOV” SS-EPI DWI in patients without significant pathology.<sup>14</sup> In the current study, we demonstrate that this technique has added clinical value to evaluate pathology in all 3 compartments of the cervical and thoracic spine, and our results suggest that there is statistically significant added value in evaluating pathologic processes such as infection, infarction, demyelination, and neoplasm. Even for cases in which a diagnosis is suggested by conventional anatomic imaging alone, this technique increased clinical confidence in the diagnosis. Adding rFOV DWI was found to be helpful in approximately a third of cases with pathology, both by narrowing the differential diagnosis and, at times, suggesting a specific diagnosis. The rFOV DWI technique was found to be of slightly greater utility in excluding pathologies than in favoring specific diagnoses. For instance, acute spinal cord infarction is often included in the differential diagnoses of intramedullary T2 hyperintensity that could also result from demyelination or contusion, among other possibilities, but it can be excluded when there is no reduced diffusion.

The addition of the rFOV DWI sequence to the clinical evaluation of spinal column MR imaging examinations did not result in an equal effect on reader evaluation across all pathologies. This finding suggests that the addition of the rFOV DWI sequence aids in the evaluation of certain pathologies (listed in Table 1) more than others. Degenerative disk disease and its many variants (including diskogenic marrow changes and disk extrusion, for example) are common and well-characterized by traditional anatomic sequences. The added tissue characterization that diffusion imaging affords does not appear necessary to make the appropriate findings, to influence the differential diagnosis, or to increase clinical confidence in the diagnosis. The observation that vascular malformations, intramedullary hemorrhage, and syrinx demonstrated no statistically significant benefit by the addition of rFOV diffusion images is likely due to the very small sample size of each of these pathologies in our patient cohort. Review of the rFOV DWI sequence at times resulted in significant narrowing of the included pathologies comprising the differential diagnosis and occasionally excluded all initially considered pathologies.

In a few select cases, unexpected findings that might otherwise have been missed were noted on the rFOV DWI sequence (eg, the small schwannomas shown in Fig 2). Similarly, Fig 4 highlights a case in which the presence of extradural blood products, while present on the conventional sequences, is more easily identified on the rFOV diffusion images. Moreover, in several cases, marked patient motion rendered the routine anatomic images nearly nondiagnostic (so that readers could not exclude the presence of several pathologic entities); following review of the rFOV DWI sequence, which is relatively resistant to motion artifacts, the readers were able to significantly narrow the diagnostic possibilities.

Table 2 includes data for the Bowker test of symmetry, which comparatively evaluates possible symmetry in score distribution between the 2 readers. With the exception of the assessment of clinical confidence on the addition of the rFOV DWI sequence (in which the P value suggests a moderate de-

Table 2: Agreement between readers				
Reader Agreement	Unweighted $\kappa$	95% CI	95% CI (P Value)	Symmetry Test (P Value)
Identify pathology	0.77	0.73–0.80	<.0001	<.0001 <sup>a</sup>
Confidence in pathology	0.57	0.50–0.64	<.0001	<.0001 <sup>a</sup>
Confidence in DWI	0.33	0.21–0.45	<.0001	.2145
Added value of DWI	0.77	0.70–0.83	<.0001	.0008 <sup>a</sup>

<sup>a</sup> Bowker symmetry test is statistically significant (implying overall higher scores by 1 reader compared with the other).

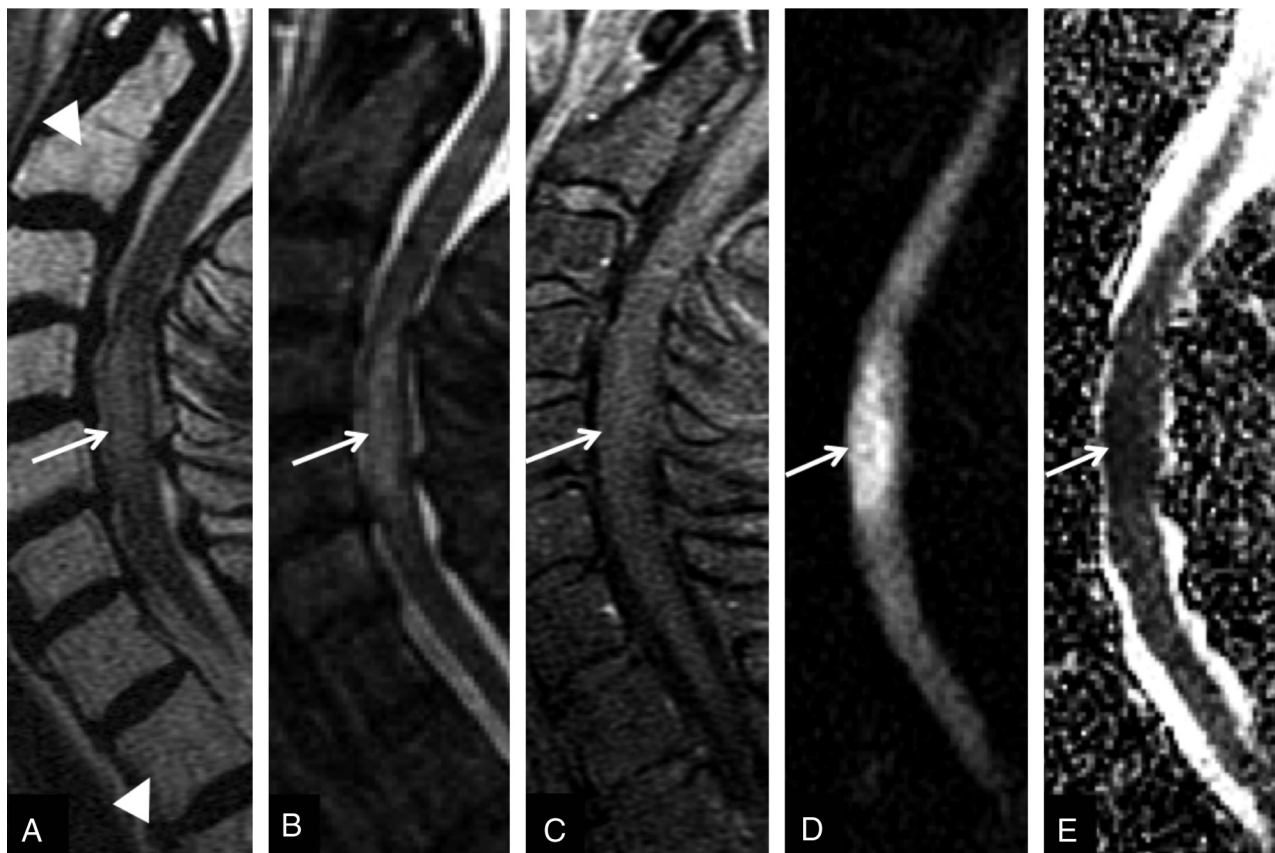


**Fig 1.** A 63-year-old man with a remote history of throat cancer and prior neck radiation, with acute onset of quadriplegia. The focal area of T2 hyperintensity (white arrows on all images) is identified at C4-C5 on the sagittal T2-weighted image (A) and STIR image (B), with no enhancement on the postgadolinium T1-weighted image (C). Increased marrow signal is present on the T2-weighted image (white arrowheads), consistent with a history of prior neck radiation. Initial diagnostic considerations might include transverse myelitis, radiation myelitis, spinal cord infarct, acute demyelination, neoplasm, and infection. On review of the sagittal rFOV DWI (D) and the corresponding ADC map (E) demonstrating reduced diffusion, readers were more confident in the diagnosis of acute cord infarct, and this was consistent with the patient's clinical course and diagnosis.

gree of symmetry in the expert reader scores), there is overall suggested asymmetry in the scores provided by the 2 expert readers, per patient examination. This asymmetry indicates that there was a reliable systematic disagreement between the 2 readers so that the  $\kappa$  values reflect not just disagreement due to measurement imprecision, but also the fact that readers may have different criteria or thresholds in identifying pathology. These results suggest that despite differing individual thresholds for identifying possible pathology (as is often true in radiologic practices), there is still statistical value in imaging the cervical and thoracic spine with the rFOV DWI technique, as evidenced by the high  $\kappa$  values representative of the readers scores for added clinical value of this sequence.

There are several limitations to our study. First, despite the large number of patients included, some rare spinal pathologies remained under-represented. For this reason, conclusions about the clinical benefit of rFOV DWI in these entities could

not be ascertained with confidence. Additionally, the study design included prespecified pathologies to aid in categorization, but it was not all-inclusive. Specific spinal pathologies that were not prospectively included in the study design but were identified on subsequent reader analysis included myelomalacia (2 cases), prevertebral hemorrhage/collection (9 cases, all in the setting of acute trauma), and vertebral congenital/segmentation anomalies (1 case of Morquio syndrome and 1 case of Klippel-Feil anomaly); rFOV DWI was not found to be of added benefit in these cases. Statistical analysis also demonstrated that 1 reader was more apt, in general, to give higher confidence ratings than the other reader. Given the relatively high  $\kappa$  values, however, this suggests that despite unequal initial grading, the overall consensus and change in assigned confidence scores of the readers were similar regarding the added benefit of the rFOV DWI sequence and likely do not impact the conclusions of the study. Finally, while the

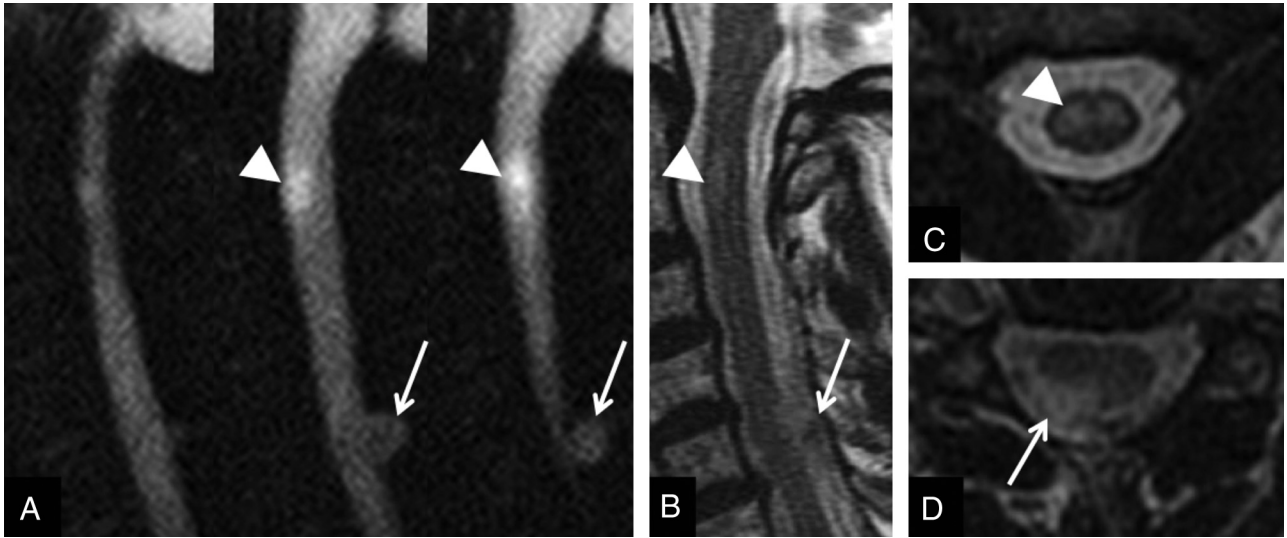


**Fig 2.** A 59-year-old woman with complex medical history including Crohn disease and pulmonary fibrosis who presented with lower extremity weakness and hyperreflexia. Three consecutive sagittal rFOV DWIs (A) demonstrate high signal in the cervical cord at the C2 level (arrowheads), confirmed centrally within the cord substance on an axial T2-weighted fast spin-echo image (C). Corresponding decreased ADC signal (not shown) and clinical presentation are most consistent with cord infarct. Additionally, an intradural extramedullary mass is noted on the last 2 sagittal rFOV DWIs (white arrows), which was difficult to appreciate on conventional sagittal (B) and axial (D) T2-weighted fast spin-echo images. While it was not biopsied, the high signal intensity of the mass on T2-weighted imaging suggests that this is likely a schwannoma.



**Fig 3.** A 19-year-old woman with new-onset back pain. rFOV DWI (A), trace ADC map (B), T2 fast-spin-echo (C), and postgadolinium T1-weighted (D) sagittal image demonstrate a hypercellular process in multiple vertebral bodies (white arrows) and the epidural space (asterisks). The complete extent of vertebral body and posterior element involvement is better defined on the rFOV DWI compared with the conventional images. Biopsy demonstrated lymphoma.

rFOV DWI technique reduced the geometric distortion associated with more traditional SS-EPI readout schemes,<sup>14</sup> it was not entirely eliminated; this distortion can still be problematic.

Continued work on artifacts reduction will clearly benefit this application for use in patients with large susceptibility variations.



**Fig 4.** A 17-year-old boy status post-assault, found to have multiple facial fractures. Sagittal anatomic images include STIR (A), T2 FSE (B), and spin-echo T1-weighted (C), and multiple axial FSE T2-weighted images (D). A retroclival and upper cervical subdural or epidural hematoma extending caudally to the C2-C3 level is far more conspicuous on the rFOV DWI (white arrow in E) than on the conventional images, where it mimics CSF flow artifact on the STIR and FSE T2-weighted images.

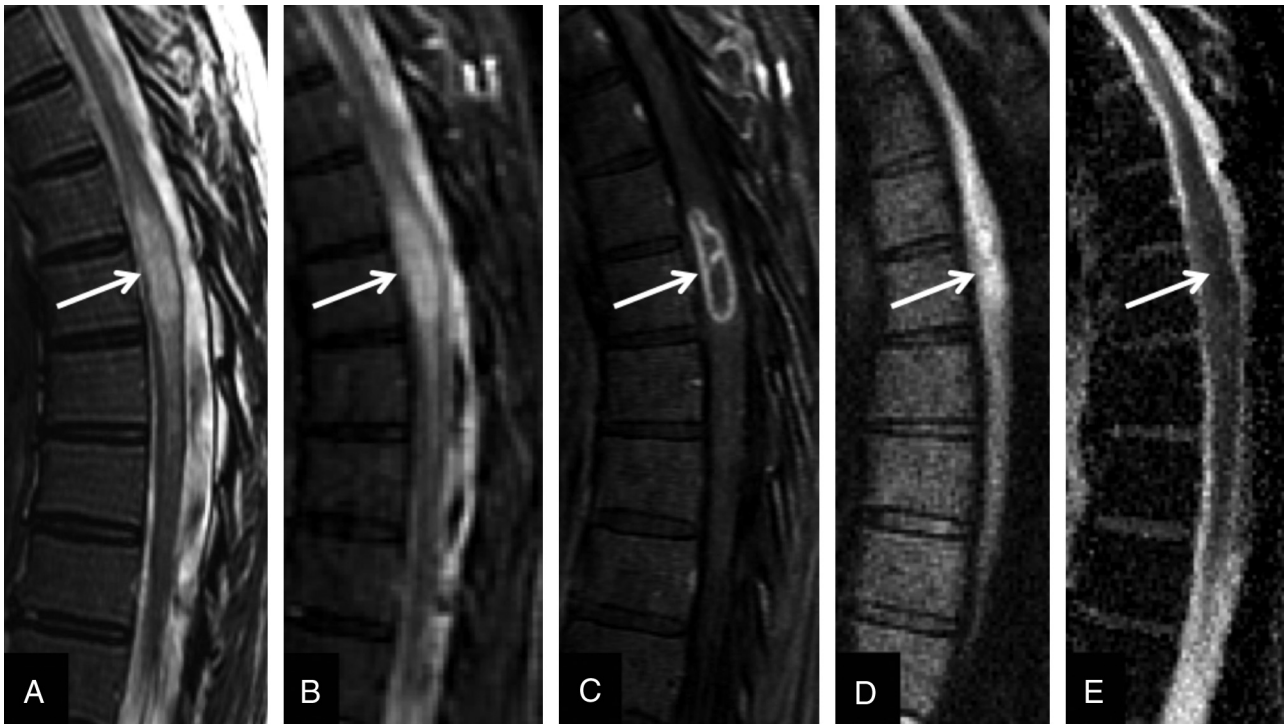


**Fig 5.** A 60-year-old woman with a history of chronic granulomatous disease and recent dental work presented to an outside hospital with left arm weakness and general malaise. An expansile focal area of T2 signal abnormality (white arrow on all images) is identified on the sagittal FSE T2-weighted image (A) and confirmed on STIR (B). Sagittal postgadolinium T1-weighted image (C) confirms a rim-enhancing intramedullary lesion, with a central nonenhancing portion. The rFOV DWI (D) demonstrates diffusion restriction centrally within this lesion, evidenced by low ADC (E), suggesting the presence of pus. This was interpreted as consistent with intramedullary abscess, and the patient responded well to antibiotics.

Finally, the prevalence of pathology at an academic center may differ significantly from that in the community and may represent an additional source of bias within this study. It is,

therefore, possible that our results overestimate the added benefit of the rFOV DWI sequence in routine imaging of the cervical and thoracic spine in a general community practice

setting, because we found no significant benefit with the addition of this sequence in the absence of pathology. Furthermore, although readers were blinded to patient identifiers and all patient data, they were not blinded to the study design; this could represent an additional source of error. The subjective nature of the rating system used and the subjective assessment of the possible presence of pathology, while commensurate with that of general radiologic interpretation, may have resulted in an overestimation of the significance and value of the rFOV DWI sequence. While we believe our results suggest that the rFOV DWI technique adds clinical utility in evaluating the cervical and thoracic spine, meaningful differences in patient outcome were not evaluated in this study and would be of benefit to further substantiate these initial results.

## Conclusions

DWI of the cervical and thoracic spine and spinal cord improved the characterization of a wide range of pathology, including demyelinating disease, acute infarction, infection, traumatic injury, and neoplasm. This study demonstrates that when applied to an unselected clinical population presenting to an academic hospital, rFOV DWI adds clinical value by helping to identify pathology, narrow the differential diagnosis, and increase clinician confidence.

Disclosures: Greg Zaharchuk—RELATED: Grant: GE Healthcare,\* Comments: research grant, UNRELATED: Consultancy: GE Healthcare Neuroradiology Advisory Board, Grants/Grants Pending: National Institutes of Health.\* Ajit Shankaranarayan—UNRELATED: Employment: GE Healthcare, Comments: full-time employee. Suchandrima Banerjee—UNRELATED: Employment: GE Healthcare. Dwight Nishimura—RELATED: Grant: GE Healthcare,\* Comments: programmatic support. Nancy Fischbein—UNRELATED: Board Membership: American Journal of Neuroradiology, Comments: Senior Editor. \*Money paid to the institution.

## References

1. LeBihan D. Molecular diffusion nuclear magnetic resonance imaging. *Magn Reson Q* 1991;7:1–30
2. Bammer R. Basic principles of diffusion-weighted imaging. *Eur J Radiol* 2003;45:169–84
3. Moseley ME, Wendland MF, Kucharczyk J. Magnetic resonance imaging of diffusion and perfusion. *Top Magn Reson Imaging* 1991;3:50–67

4. Holder CA. MR diffusion imaging of the cervical spine. *Magn Reson Imaging Clin N Am* 2000;8:675–86
5. Melhem ER. Technical challenges in MR imaging of the cervical spine and cord. *Magn Reson Imaging Clin N Am* 2000;8:435–52
6. Bammer R, Fazekas F. Diffusion imaging of the human spinal cord and the vertebral column. *Top Magn Reson Imaging* 2003;14:461–76
7. Bammer R, Augustin M, Prokesch RW, et al. Diffusion-weighted imaging of the spinal cord: interleaved echo-planar imaging is superior to fast spin-echo. *J Magn Reson Imaging* 2002;15:364–73
8. Clark CA, Barker GJ, Tofts PS. Magnetic resonance diffusion imaging of the human cervical spinal cord in vivo. *Magn Reson Med* 1999;41:1269–73
9. Zhang J, Huan Y, Qian Y, et al. Multishot diffusion-weighted imaging features in spinal cord infarction. *J Spinal Disord Tech* 2005;18:277–82
10. Bammer R, Stollberger R, Augustin M, et al. Diffusion-weighted imaging with navigated interleaved echo-planar imaging and a conventional gradient system. *Radiology* 1999;211:799–806
11. Cercignani M, Horsfield MA, Agosta F, et al. Sensitivity-encoded diffusion tensor MR imaging of the cervical cord. *AJNR Am J Neuroradiol* 2003;24:1254–56
12. Tsuchiya K, Fujikawa A, Suzuki Y. Diffusion tractography of the cervical spinal cord by using parallel imaging. *AJNR Am J Neuroradiol* 2005;26:398–400
13. Holdsworth SJ, Skare S, Newbould RD, et al. Readout-segmented EPI for rapid high resolution diffusion imaging at 3 T. *Eur J Radiol* 2008;65:36–46
14. Zaharchuk G, Saritas EU, Andre JB, et al. Reduced field-of-view diffusion imaging of the human spinal cord: comparison with conventional single-shot echo-planar imaging. *AJNR Am J Neuroradiol* 2011;32:813–20
15. Jeong EK, Kim SE, Guo J, et al. High-resolution DTI with 2D interleaved multisllice reduced FOV single-shot diffusion-weighted EPI (2D ss-rFOV-DWEPI). *Magn Reson Med* 2005;54:1575–79
16. Saritas EU, Cunningham CH, Lee JH, et al. DWI of the spinal cord with reduced FOV single-shot EPI. *Magn Reson Med* 2008;60:468–73
17. Wilm BJ, Svensson J, Henning A, et al. Reduced field-of-view MRI using outer volume suppression for spinal cord diffusion imaging. *Magn Reson Med* 2007;57:625–30
18. Eguchi Y, Ohtori S, Yamashita M, et al. Diffusion magnetic resonance imaging to differentiate degenerative from infectious endplate abnormalities in the lumbar spine. *Spine* 2011;36:E198–202
19. Chan JH, Peh WC, Tsui EY, et al. Acute vertebral body compression fractures: discrimination between benign and malignant causes using apparent diffusion coefficients. *Br J Radiol* 2002;75:207–14
20. Zhou XJ, Leeds NE, McKinnon GC, et al. Characterization of benign and metastatic vertebral compression fractures with quantitative diffusion MR imaging. *AJNR Am J Neuroradiol* 2002;23:165–70
21. Maeda M, Sakuma H, Maier SE, et al. Quantitative assessment of diffusion abnormalities in benign and malignant vertebral compression fractures by line scan diffusion-weighted imaging. *AJR Am J Roentgenol* 2003;181:1203–09
22. Tang G, Liu Y, Li W, et al. Optimization of b value in diffusion-weighted MRI for the differential diagnosis of benign and malignant vertebral fractures. *Skeletal Radiol* 2007;36:1035–41
23. Balliu E, Vilanova JC, Pelaez I, et al. Diagnostic value of apparent diffusion coefficients to differentiate benign from malignant vertebral bone marrow lesions. *Eur J Radiol* 2009;69:560–66